Malaysian Journal of Analytical Sciences (MJAS)
Published by Malaysian Analytical Sciences Society

SYNTHESIS, CRYSTAL STRUCTURE, SPECTROSCOPIC CHARACTERISATION, AND PHOTOPHYSICAL PROPERTIES OF IRIDIUM(III) COMPLEX WITH PYRIDINE-FORMIMIDAMIDE ANCILLARY LIGAND

(Sintesis, Struktur Hablur, Pencirian Spekroskopi, dan Sifat Fotofizikal Kompleks Iridium(III) dengan Ligan Ansilari Piridina-Formimidamida)

Nurul Husna As Saedah Bain[1], Noorshida Mohd Ali[1,*], Yusnita Juahir[1], Suzaliza Mustafar[1], Mohammad Kassim[2], Saifful Kamaluddin Muzakir@Lokman[3], Bohari Mohd Yamin[2], and Jean-Claude Daran[4]

[1]*Chemistry Department,*
Faculty of Science and Mathematics,
Universiti Pendidikan Sultan Idris,
35900, Tanjong Malim, Perak, Malaysia
[2]*School of Chemical Sciences and Food Technology,*
Faculty of Science and Technology,
Universiti Kebangsaan Malaysia, 43600 Bangi, Selangor, Malaysia
[3]*Faculty of Industrial Sciences and Technology,*
Universiti Malaysia Pahang,
26300 Gambang, Pahang, Malaysia
[4]*CNRS, LCC (Laboratoire de Chimie de Coordination),*
Université de Toulouse,
UPS, INPT, 205, Route de Narbonne, F-31077 Toulouse, France

[*]*Corresponding author: noorshida@fsmt.upsi.edu.my*

Received: 11 November 2022; Accepted: 17 January 2023; Published: 19 April 2023

Abstract

A phosphorescent Ir(III) complex was synthesised between 2-(1*H*-1,2,4-triazol-1-yl)pyridine and Ir(III) dimer, $[Ir(2,4\text{-}F_2ppy)_2(\mu\text{-}Cl)]_2$, where ppy denotes 2-phenylpyridine by reflux method. The Ir(III) complex was fully characterised by FTIR, NMR, LC-MS, and UV-Vis absorption spectroscopic methods. The presence of a strong band at 2220 cm^{-1} due to ν(C≡N) was revealed by the IR analysis. Both pyridine and phenyl aromatic rings have C=N stretching band at 1598 cm^{-1} and C=C stretching bands at 1554 and 1400 cm^{-1}, respectively. The ^1H NMR spectrum showed signals in the aromatic range of δ 5.00–9.00 ppm corresponding to phenylpyridine protons. The ^{13}C NMR spectroscopic data were consistent with the Ir(III) complex formula, which revealed 37 carbon signals. The Ir(III) complex displayed the ESI-MS spectrum at m/z = 823. The UV-Vis spectrum displayed a weaker and broader band (374 nm) in the visible region due to the spin-forbidden ^{3}MLCT transitions. The X-ray crystallographic study revealed that the Ir(III) ion was coordinated to the pyridine-formimidamide ancillary ligand and two 2-(2,4-difluorophenyl)pyridine cyclometalating ligands in an octahedral geometry. Steady-state emission spectroscopy determined that

the Ir(III) complex emitted blue-green light in dichloromethane solution at room temperature with the vibronic structure to the peak shape (λ = 462 nm and 487 nm) due to the admixture of ^{3}LC and ^{3}MLCT character excited states.

Keywords: Ir(III) complex, formimidamide, ancillary ligand, phosphorescent, metal-to-ligand charge transfer

Abstrak

Kompleks Ir(III) berpendar fosfor disintesis antara 2-(1*H*-1,2,4-triazola-1-yl)piridina dan dimer Ir(III), [Ir(2,4-F_2ppy)$_2$(μ- Cl)]$_2$ di mana ppy mewakili 2-fenilpiridina melalui kaedah refluks. Kompleks Ir(III) dicirikan sepenuhnya melalui kaedah spektroskopi: FTIR, NMR, LC-MS, dan penyerapan UV-Vis. Kehadiran satu jalur kuat pada 2220 cm^{-1} disebabkan oleh ν(C≡N) telah dikenal pasti daripada analisis IR. Kedua-dua gelang aromatik piridina dan fenil, masing-masing mempunyai jalur regangan C=N pada 1598 cm^{-1} dan jalur regangan C=C pada 1554 dan 1400 cm^{-1}. Spektrum ^{1}H NMR menunjukkan isyarat dalam julat aromatik δ 5.00–9.00 ppm sepadan dengan proton fenilpiridina. Data spektroskopi ^{13}C NMR juga konsisten dengan formula kompleks Ir(III), yang menunjukkan 37 isyarat karbon. Kompleks Ir(III) menunjukkan spektrum ESI-MS pada m/z = 823. Spektrum UV-Vis mempamerkan jalur yang lebih lemah dan lebar (374 nm) di rantau yang boleh dilihat disebabkan oleh peralihan ^{3}MLCT spin-terlarang. Kajian kristalografi sinar-X menunjukkan ion Ir(III) dikoordinasi kepada ligan ansilari piridina-formimidamida dan dua ligan siklometalasi 2-(2,4-diflorofenil)piridina dalam geometri oktahedral. Spektroskopi pancaran keadaan-stabil menunjukkan kompleks Ir(III) memancarkan cahaya biru-hijau dalam larutan diklorometana pada suhu bilik dengan struktur vibronik kepada bentuk puncak (λ = 462 nm dan 487 nm) disebabkan oleh bauran ciri keadaan teruja ^{3}LC dan ^{3}MLCT.

Kata kunci: Kompleks Ir(III), Formimidamida, ligan ansilari, berpendar fosfor, pemindahan cas logam ke ligan

Introduction

Phosphorescent transition metal complexes have attracted increased scientific interest because they are widely used in organic light-emitting diodes (OLEDs) for next-generation lighting sources and flat-panel displays [1,2]. The spin-orbit coupling of phosphorescent transition metal complexes has been used to access the triplet excitons that fluorescent emitters previously could not reach [3,4]. Ir(III) complexes are considered to be the most promising triplet harvester because of their high phosphorescence quantum efficiencies, short phosphorescence lifetimes, and colour-tuning flexibility [5–7]. Blue OLEDs are the most severe research issues compared to red- and green-emitting materials [8,10]. In this regard, the design and synthesis of deep-blue-emitting Ir(III) complexes are challenging. Although high quantum efficiencies (QEs) exceeding 30% have been achieved for green and red OLED devices, high QEs for deep-blue OLED devices have rarely been reported because blue phosphors have faster decomposition due to their highly energetic excited states [7].

It has been found that there are numerous ways to change the emission colour of a variety of heteroleptic Ir(III) complexes with cyclometalated phenylpyridine ligands. One of the most promising techniques to produce the emission to blue is to substitute the cyclometalating ligand with an electron-withdrawing group, such as a fluorine atom that will stabilise the highest occupied molecular orbital (HOMO) orbitals that are localised on the phenyl ring and the metal atom [7,9]. Additionally, the inclusion of novel chelating ligands as ancillary ligands can lower the lowest unoccupied molecular orbital (LUMO) level [9], increasing the HOMO-LUMO energy gap. Therefore, to have stable efficiencies of blue emitters for OLEDs, Ir(III) complex must have a sufficiently large energy difference between HOMO and LUMO [7–10]. In this report, we presented the use of novel pyridine-formimidamide as the ancillary ligand for Ir(III) complex and detailed explanation of the synthesis, spectroscopic, and X-ray crystallographic analysis studies.

Materials and Methods

Materials

Unless otherwise specified, all chemicals were obtained from various sources and used exactly as obtained.

Physical measurements

Elemental analysis for carbon (C), hydrogen (H), and nitrogen (N) was performed using a CHNS-O elemental analyser model Flash EA 1112 Series. ^{1}H NMR and ^{13}C

NMR spectra using deuterated dichloromethane (CD_2Cl_2) as solvent were analysed by a nuclear magnetic resonance (NMR) spectrometer (JNM-ECX-500, JEOL). At room temperature, the IR spectrum from a Thermo Nicolet 6700 spectrometer was acquired in the 4000–500 cm^{-1} range. The mass spectrum was analysed by a liquid chromatography-mass spectrometer (LC-MS) model 6490 Triple Quadrupole, Agilent Technologies. The column used was a Phenomenex Gemini NX (C_{18}, 150 × 2.0 mm, ID 5.0 µm). The sample was prepared by dissolving 10 mg in 10 mL of acetonitrile and injected using the gradient ratio of acetonitrile and formic acid as the eluent. A Cary 60 UV-Vis spectrophotometer (Agilent Technologies) was used to analyse the UV-Vis absorption spectra in methylene chloride solution.

A photoluminescence spectrometer model FLS920 (Edinburgh Instrument) was used to obtain the steady-state emission spectrum and time-resolved fluorescence lifetime from an air-equilibrated dichloromethane solution at 298 K. Fluorescence quantum yield was measured by relative method using *tris*(2-phenylpyridine)iridium(III), $Ir(ppy)_3$ in dichloromethane solution ($\Phi = 0.4$) as the standard [11]. The equation $\Phi_s = \Phi_r(I_s/I_r)(A_r/A_s)(\eta_s^2/\eta_r^2)$ was used to calculate the quantum yield, where, Φ_s is the quantum yield of the sample, Φ_r is the quantum yield of the reference, I_s is the area of the emission fluorescence spectrum of the sample, I_r is the area of the emission fluorescence spectrum of the reference, A_s is the absorbance of the sample, A_r is the absorbance of the reference, η_s is the refractive index of the solvent for the sample, and η_r is the refractive index of the solvent for the reference.

Synthesis

Chloro-bridged iridium(III) dimer (0.0605 g, 0.1 mmol equiv.), 2-[4-(4-methyl-benzyl)-[1,2,4]triazol-1-yl]-pyridine ligand (0.0289 g, 0.25 mmol equiv.), and silver(I) oxide (0.0290 g, 0.21 mmol equiv.) in 15 mL of 1,2-dicholoroethane were refluxed in the dark and under an N_2 atmosphere for 24 h. The solution was collected by filtering through celite after it had cooled to room temperature. Then, the solution was dried over anhydrous sodium sulphate and purified with dichloromethane/methanol (90:10 v/v) solvent. The column yielded a yellowish product.

Yield: 69%. ^{1}H NMR (500 MHz, CD_2Cl_2): δ 8.21 (d, J = 8.6 Hz, 2H), 7.73 (t, J = 7.7 Hz, 1H), 7.67 (d, J = 2.3 Hz, 1H), 7.61 (t, J = 7.2 Hz, 1H), 7.49 (t, J = 8.0 Hz, 1H), 7.42 (t, J = 5.7 Hz, 1H), 7.35 (t, J = 4.0 Hz, 1H), 6.94–6.88 (m, 4H), 6.66 (t, J = 6.0 Hz, 1H), 6.46–6.42 (m, 2H), 6.28 (t, J = 11.5 Hz, 1H), 5.67 (d, J = 2.3 Hz, 1H), 5.65 (d, J = 2.3 Hz, 1H), 5.59 (t, J = 6.3 Hz, 1H), 4.88 (d, J = 14.3 Hz, 1H), 2.26 (s, 5H). ^{13}C NMR (126 MHz, CD_2Cl_2): δ 172.0, 165.3, 165.3, 165.0, 164.9, 164.5, 164.4, 162.9, 162.8, 162.5, 162.4, 160.7, 160.6, 154.5, 148.6, 147.7, 139.6, 137.8, 136.6, 133.6, 128.9, 127.7, 127.0, 123.7, 123.6, 123.4, 123.1, 123.0, 122.0, 118.2, 117.9, 112.7, 112.5, 98.4, 96.3, 20.8. FTIR (ATR, ν/cm^{-1}): 3077 (w, ν(C–$H_{aromatic}$)), 2925 (w, ν(C–H_{alkyl})), 2220 (s, ν(C≡$N_{nitrile}$)), 1600–1400 (s, ν(C=$C_{aromatic}$); s, ν(C=N_{py})), 1244 (s, ν(C–N)); 830–720 (s, δ(C–$H_{ortho/para\ out\text{-}of\text{-}plane}$); 1100–984 (s, δ(C–$H_{ortho/para\ in\text{-}plane}$). LC-MS (ESI, m/z): 823 [M+H] (calc. 822). Anal. calcd. for $C_{37}H_{25}N_6F_4Ir$: C, 54.07; H, 3.07; N, 10.23%. Found: C, 53.53; H, 3.46; N, 9.27%.

X-ray crystallographic analysis

Single crystal X-ray crystallographic study was performed using a Bruker D8 QUEST with a PHOTON III charge- integrating pixel array detector area-detector diffractometer (Bruker, AXS Inc., Madison, WI, USA) and graphite-monochromated Mo-Kα radiation (λ = 0.71073 Å). The data collected were reduced using the SAINT [12] programme, and empirical absorption correction was carried out using SADABS [12]. The structure was solved by direct methods and refined via a SHELXTL [13] software package using a full-matrix least-squares approach. The molecular graphics were created using SHELXTL software. All hydrogen atoms were assigned by assuming idealised geometries with d(C–H) = 0.93 and 0.96 Å for aromatic and aliphatic, respectively, with Uiso(H) = 1.2 Ueq(C). All non-hydrogen atoms were refined anisotropically. The PLATON programme was used for molecular structure calculation [14]. The ellipsoids of one Cl of the dichloromethane are relatively elongated, suggesting a disorder; however, any attempt to split the position of the Cl failed. Hence, it is kept as it is (Figure 3).

Results and Discussion

The chloro-bridged iridium(III) dimer, [Ir(2,4-F_2ppy)$_2$(μ-Cl)]$_2$ (F_2ppy = difluorophenylpyridine), was synthesised by reacting $IrCl_3 \cdot nH_2O$ with 2-(2,4-difluorophenyl)pyridine in a refluxed 2-ethoxylethanol/water (3:1) under an N_2 atmosphere [15] and was then used in the subsequent reaction without further purification. The previously synthesised ligand, (2-(4-methylbenzyl)-1*H*-1,2,4-triazol-1-yl)pyridine (mbpyta) [16], was refluxed with [Ir(2,4-F_2ppy)$_2$(μ-Cl)]$_2$ to give [Ir(2,4-F_2ppy)$_2$(mbpyf)] (69%). Scheme 1 depicts the schematic process leading to [Ir(2,4-F_2ppy)$_2$(mbpyf)], including the silver carbene-complex intermediate. The difficulty and challenge of separating the pure product from the crude mixture during the purification stage prevented the yield of the synthesised Ir(III) complex from reaching 80% and above. The elemental analysis of [Ir(2,4-F_2ppy)$_2$(mbpyf)] complex matched the suggested chemical formula. In addition, the electrospray mass spectrometry (ESMS) spectrum of the [Ir(2,4-F_2ppy)$_2$(mbpyf)] complex was recorded to determine the molecular species in the solution (Figure S1). The observed pattern of the ESMS spectrum, which displayed a peak at m/z = 823, complemented the calculated one, suggesting that the structure of the species was [Ir(2,4-F_2ppy)$_2$(mbpyf)] + H].

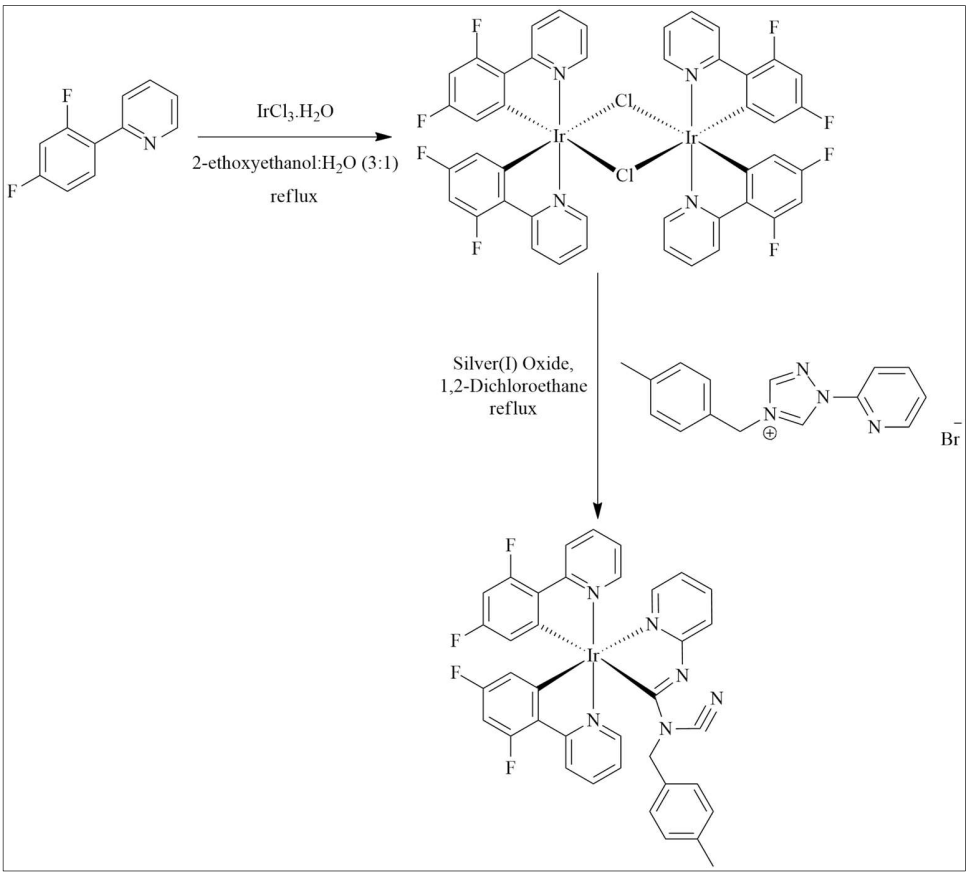

Scheme 1. Schematic reaction pathway and chemical structures of chloro-bridged iridium(III) dimer and [Ir(2,4-F_2ppy)$_2$(mbpyf)] complex

Figure 1 depicts the IR spectrum of the [Ir(2,4-F_2ppy)$_2$(mbpyf)] complex. A strong, significant band that can be observed at 2220 cm^{-1} is due to ν(C≡N), which resembles the predictable pattern for the nitrile group [17]. The C=N stretching band appeared at 1598 cm^{-1} [18] and C=C stretching bands appeared in two absorption bands at 1554 and 1400 cm^{-1} [19], respectively, indicating the presence of aromatic rings of

pyridine and phenyl [18]. Furthermore, a strong band was detected at 1244 cm^{-1}, representing ν(C–N). The typical weak ν(C–H) in aromatic phenyl and pyridine rings was observed at 3077 cm^{-1}, while the stretching bands for (C–H) in alkyl are shown in the spectral region of 2981–2925 cm^{-1}. Additionally, strong bending bands of (C–H) were observed in the range of 830–720 cm^{-1} for ortho/para out-of-plane and in the region of 1100–984 cm^{-1} for ortho/para in-plane substituents on the aromatic ring [17,18].

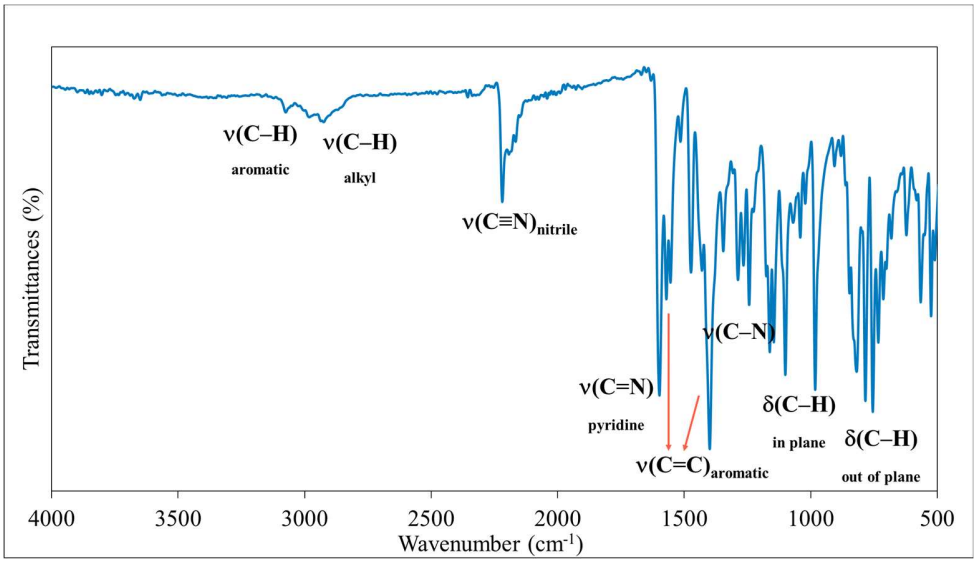

Figure 1. IR spectrum of [Ir(2,4-F_2ppy)$_2$(mbpyf)] complex

The structure of the [Ir(2,4-F_2ppy)$_2$(mbpyf)] complex was further investigated using NMR spectroscopy. The ^{1}H NMR and ^{13}C NMR spectra were recorded in deuterated dichloromethane (CD_2Cl_2) and are presented in Figures 2 and S2, respectively. Based on the HMQC spectrum, the proton resonances of the [Ir(2,4-F_2ppy)$_2$(mbpyf)] complex were assigned and compared to the ^{1}H NMR spectra of its iridium(III) dimer and ligand mbpyta in Figures S3 and S4, respectively. The aromatic signals appeared between 8.30 and 4.90 ppm, correlating to the phenylpyridine protons [6]. In addition, as expected, the signal of two singlet peaks for the mbpyta proton disappeared after deprotonation and coordination of the ancillary ligand. The multiplet signals in the aliphatic region at 2.25 ppm are caused by methylene protons at H13 and H14, together with methyl substitution groups at H19, H20, and H21 [17,18]. Hydrogen and fluorine (spin ½) have extremely strong coupling; thus, the interaction with two fluorine nuclei causes the proton signals of H5 and H5' to divide into a multiplet, while H6 and H6' split into triplets [17,18].

Furthermore, the ^{13}C NMR spectrum assisted in the structural identification of [Ir(2,4-F_2ppy)$_2$(mbpyf)]. Three distinct peaks can be ascribed to –CH_3 (20.8 ppm), –CH_2– (20.9 ppm), and C≡N (128.9 ppm) [17,18], while the other 34 significant carbon signals appeared between 96.3 and 172.0 ppm, corresponding to the number of carbon atoms in aromatic regions, consistent with the low-symmetry structure. According to Barnard and Hogan, aromatic carbon bonded to a nitrogen atom can be seen at approximately over 150 ppm, while aromatic carbon attached to a fluorine atom was found between 90 and 100 ppm [20]. Four –CF peaks appeared at 98.6, 98.4, 96.4, and 96.3 ppm, while six peaks of –C=N aromatic appeared at 162.9, 162.8, 162.5, 162.4, 160.7, and 160.6 ppm. However, a peak at 172.0 ppm ascribed to the –N–C=N bonded to the iridium atom showing a deshielded effect to the lower field of ^{13}C NMR spectrum due to the substantial electron donor effect contributed by the formimidamide ligand [21].

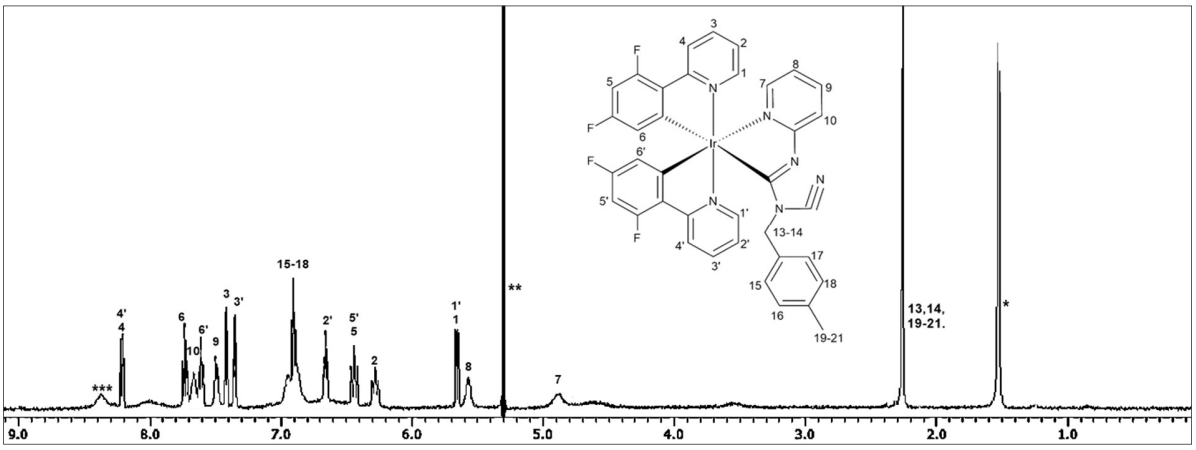

Figure 2. ^{1}H-NMR spectrum for [Ir(2,4-F_2ppy)$_2$(mbpyf)] complex in deuterated CD_2Cl_2 with its labelling scheme, H_2O is marked with *, residual solvent is marked with **, and impurity is marked with ***.

Crystal structure

Slow diffusion of hexane into a dichloromethane solution of [Ir(2,4-F_2ppy)$_2$(mbpyf)] resulted in single crystals of the compound. Despite the challenge of getting high-quality crystals, a single yellow crystal was chosen and put on a glass fibre before data collection. The [Ir(2,4-F_2ppy)$_2$(mbpyf)] complex crystallised in a monoclinic system with space group $P2_1/n$, a = 11.2164(4) Å, b = 15.5922(4) Å, c = 20.8074(7) Å, α = 90.0°, β = 91.098(2)°, γ = 90.0°, Z = 4, and V = 3638.3(2) Å^3. Table 1 presents the crystal system and refinement parameters. The ORTEP diagram of the [Ir(2,4-F_2ppy)$_2$(mbpyf)] complex with the solvated dichloromethane molecule is shown in Figure 3. Atomic coordinates and equivalent isotropic and anisotropic displacement parameters for [Ir(2,4-F_2ppy)$_2$(mbpyf)] are listed in Tables S5 and S6, respectively.

The structure of the [Ir(2,4-F_2ppy)$_2$(mbpyf)] complex is depicted in Figure 3. Two difluorophenylpyridine ligands are coordinated to the central Ir1 atom through their two pyridyl N and two phenylated C atoms, while one (2-(4-methylbenzyl)-pyridine-2-yl)formimidamide ligand is coordinated to the central Ir1 atom through its N and C atoms in a bidentate manner. The geometry of the Ir(III) complex is a distorted octahedron. The C12 and N3 atoms occupy the axial position with C12–Ir1–N3 bond angle of 176.03(12)°. The other trans atoms occupy the equatorial position with N1–Ir1–N2 and C1–Ir1–C26 bond angles of 173.08(13)° and 168.87(14)°, respectively. The steric structure of the ligands plays a significant role in the complex's distorted nature [22]. The *cis* angles about the central Ir atom are between 80.06(17)° and 96.30(13)°. The axial C12–Ir1 and N3–Ir1 are 2.017(4) Å and 2.122(4) Å, respectively. The fact that the axial N3–Ir1 bond length (2.122(4) Å) is a little bit longer than the other *trans*–oriented Ir1–N bonds (Table 2) implies that there is only weak coordination between the ancillary ligand and the central metal [23]. Other relevant bond angles and lengths are shown in Table 2. Both difluorophenylpyridine ligands are coordinated to the central Ir1 atom and give planar planes of Ir1/F1/F2/N1/(C1–C11) and Ir1/F3/F4/N2/(C12–C22) with a maximum deviation of 0.046(4) Å for C1 atom and 0.108(1) Å for Ir1 atom from the least square plane, respectively. The dihedral angle between the two planes is 79.51(7)°. The Ir1/N3/N4/N5/N6/C12/(C23–C29) fragment of the third ligand is also planar with a maximum deviation of 0.106(5) Å for the C12 atom from the least square plane. The plane makes dihedral angles of 88.96(7) ° and 89.85(8)° with the fluoropyridyl Ir1/F1/F2/N1/(C1–C11) and Ir1/F3/F4/N2/(C12–C22) planes, respectively. The cyclometallated carbon atoms C11 and C12, which are *cis* to one another, showed approximately the same distances from Ir1 (2.055(4) Å and 2.017(4) Å), which are similar to many analogous cyclometallated Ir(III) complexes [24]. The C29–N6 bond length of 1.13(9) Å indicates the presence of the nitrile triple bond functionality [6].

Table 1. Crystal data and refinement parameters for [Ir(2,4-F_2ppy)$_2$(mbpyf)] complex

Chemical formula	$IrC_{38}H_{27}Cl_2F_4IrN_6$	
Formula weight / gmol^{-1}	906.75	
Temperature / K	303(2)	
Wavelength / Å	0.71073	
Crystal system	Monoclinic	
Space group	P 2_1/n	
Unit cell dimensions / Å	a = 11.2164(4)	α = 90°
	b = 15.5922(4)	β = 91.098(2)°
	c = 20.8074(7)	γ = 90°
Volume / Å^3	3,638.3(2)	
Z	4	
Density (calculated) / Mgm^{-3}	1.655	
Absorption coefficient / mm^{-1}	3.874	
F(000)	1776	
Crystal size / mm^3	0.800 × 0.230 × 0.200	
θ range / °	2.790–28.452	
Ranges of index	$-14 \leq h \leq 15$, $-20 \leq k \leq 20$, $-27 \leq l \leq 27$	
Reflections collected	190,723	
Independent reflections	9,116 [R(int) = 0.1606]	
Completeness to theta = 25.242°	99.90%	
Method of refinement	Full-matrix least-squares on F^2	
Data / restraints / parameters	9,116 / 0 / 461	
Goodness-of-fit on F^2	1.093	
Final R indices [$I > 2\sigma(I)$]	R_1 = 0.0433, wR_2 = 0.1458	
R indices (all data)	R_1 = 0.0610, wR_2 = 0.1567	
Coefficient of extinction	n/a	
Largest diff. peak and hole / e Å^{-3}	5.519 and –1.004	

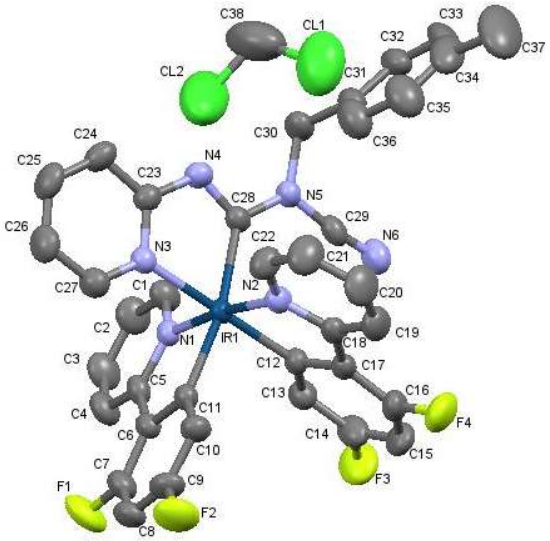

Figure 3. ORTEP diagram of the [Ir(2,4-F_2ppy)$_2$(mbpyf)] complex solvated with dichloromethane, with the numbering scheme drawn at 50% probability ellipsoid

Table 2. Selected bond lengths (Å) and angles (°) for [Ir(2,4-F_2ppy)$_2$(mbpyf)] complex

Ir1–C12	2.017 (4)	C12–Ir1–N1	93.92 (17)
Ir1–C11	2.055 (4)	C12–Ir1–N2	80.06 (17)
Ir1–N2	2.043 (4)	C12–Ir1–C11	84.83 (8)
Ir1–N1	2.043 (4)	C12–Ir1–C28	106.29 (18)
Ir1–N3	2.122 (4)	N1–Ir1–C11	79.98 (16)
Ir1–C28	2.074 (4)	N2–Ir1–C11	96.03 (16)
C28–N4	1.325(6)	N1–Ir1–C28	95.92 (16)
C28–N5	1.411(6)	N2–Ir1–C28	88.99 (16)
C29–N6	1.134(7)	N1–Ir1–N3	89.61 (14)
C28–Ir1–N3	75.25 (16)	N2–Ir1–N3	96.30 (15)
C11–Ir1–N3	94.37 (16)		

Photophysical study

Figure 4 illustrates the UV-Vis absorption spectrum of [Ir(2,4-F_2ppy)$_2$(mbpyf)] complex in a dichloromethane solution at room temperature. Most cyclometallating Ir(III) complexes have a two-part spectra absorbance pattern, with the weak intensity absorbance at the longer wavelength being associated with metal-to-ligand charge-transfer (MLCT) transitions [dπ(M)-π*(L)] near the visible region, while the shorter wavelength is attributed to spin-allowed singlet ligand-centred, ^{1}LC (π-π*) transitions of the ligands within the range of ultraviolet spectra [23–26]. The presence of phenylpyridine ligands was revealed by the intense absorption peak at 262 nm (ε = 30769.23 $M^{-1}cm^{-1}$), which is comparable to other cyclometallated Ir(III) complexes [5–9]. This peak is in the same region of the absorption spectrum as the free mbpyta ligand [16]. In addition, instead of the Gaussian form, the commonly weak, broad, and unstructured peaks due to the strong intersystem crossing by the triplet (T_1) and singlet (S_1) excited states that are driven through the central metal of an iridium atom appeared (315 nm, ε = 11031.90 $M^{-1}cm^{-1}$; 342 nm, ε = 8847.05 $M^{-1}cm^{-1}$; 374 nm, ε = 6102.56 $M^{-1}cm^{-1}$). These absorbances are related to ^{1}MLCT (ε > 10700 $M^{-1}cm^{-1}$), and ^{3}MLCT (ε ≈ 1,000–

6,000 $M^{-1}cm^{-1}$) transitions near the visible region [25–29]. Furthermore, a weak broad absorption peak at 446 nm (ε = 637.57 $M^{-1}cm^{-1}$) as a result of vibronic coupling is ascribed to the d-d transition of octahedral complexes that are forbidden due to symmetry according to the Laporte rules. However, this d-d transition band absorption is less intense than the charge transfer transition. Except for the LC transition, all these peaks are absent from the free mbpyta ligand absorption spectrum [16].

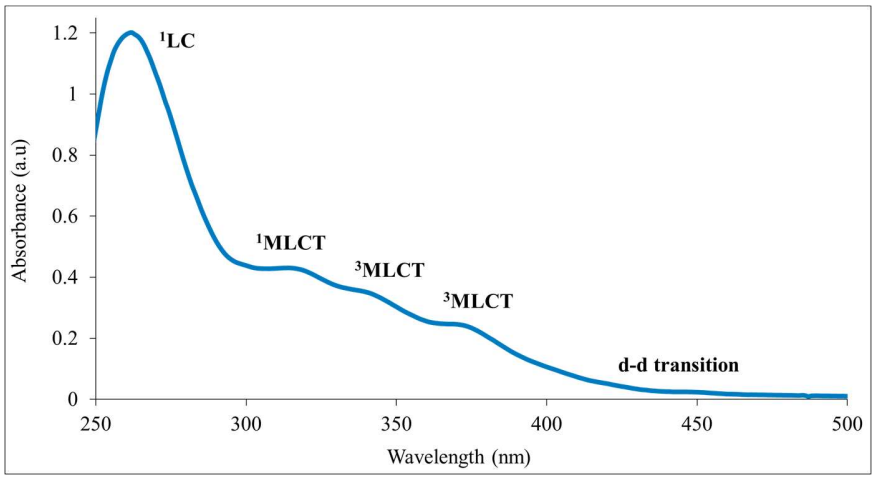

Figure 4. UV-Vis absorption spectrum of [Ir(2,4-F_2ppy)$_2$(mbpyf)] complex in a dichloromethane solution (39 μM) at 298 K labelled with the transition according to their molar absorption coefficient (ε) [30]

In Ir(III) complexes, the HOMO region is primarily metal-based and partially based on the phenyl moieties of the two phenylpyridine ligands. The photoluminescence is triggered by the excitation of an electron from the HOMO to a ligand-based π*antibonding orbital [31]. Upon excitation at λ_{ex} = 374 nm, in an air-equilibrated dichloromethane solution, the [Ir(2,4-F_2ppy)$_2$(mbpyf)] complex emits blue-green light and has a vibronic structure that reaches its peak at 298 K (Figure 5). The most visible peak is at 487 nm, while the peak at 462 nm appears as a less intense shoulder, similar to earlier Ir(III) complexes [8]. Therefore, this emission is ascribed to a transition that contains admixtures of excited states with ^{3}LC and ^{3}MLCT characters [8]. The complex's HOMO energy decreased due to the effect of the electron-withdrawing group, fluorine atoms at the 2 and 4 positions of the phenyl ring, which is *meta* with respect to the orthometallated carbon atom [30]. Furthermore, the pyridine-formimidamide auxiliary ligand is expected to increase LUMO energy, hence increasing the band gap. Thus, the emission energy of this Ir(III) complex increased and emitted blue-green light under UV light. At room temperature, the [Ir(2,4-F_2ppy)$_2$(mbpyf)] complex's emission decay time was calculated to be 29.51 ns, which is a shorter decay time compared to other cyclometallated iridium(III) complexes like FIrpic [28]. The influence of the 5d-electron densities of the iridium centre on the HOMO results in a short triplet lifetime [31]. In dichloromethane solution, the phosphorescence quantum yield (ΦP) is 0.37 compared to *fac*-Ir(ppy)$_3$ (ΦP = 0.40), and the radiative and non-radiative rate constants are 12.5 × 10^5 s^{-1} and 21.4 × 10^5 s^{-1}, respectively.

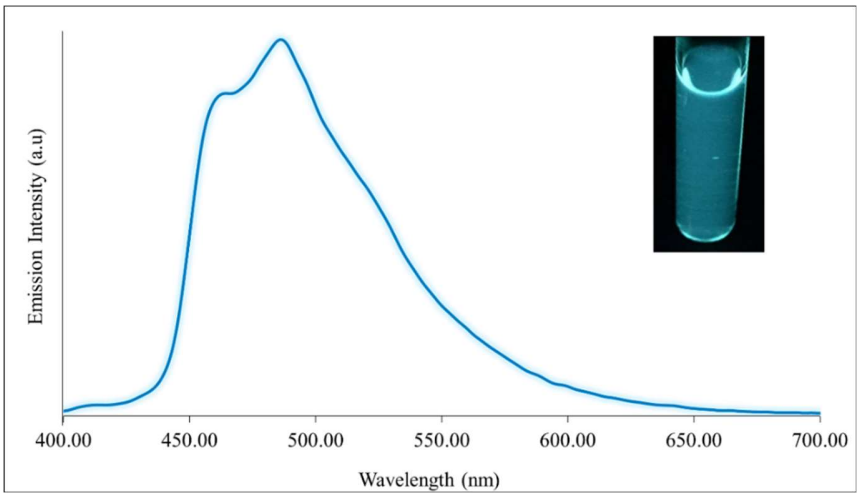

Figure 5. The emission spectrum of [Ir(2,4-F_2ppy)$_2$(mbpyf)] complex in air-equilibrated dichloromethane solution (39 μM) at 298 K. Inset: Luminescence photo of Ir(III) complex in CH_2Cl_2 under UV light

Conclusion

Ir(III) complex bearing pyridine-formimidamide ancillary ligand was successfully synthesised in good yield, characterised by spectroscopic methods, exhibited almost blue emission (λ_{em} = 464 nm) at room temperature, with phosphorescence quantum yield (Φ_p) of 0.37. The crystal structure of the Ir(III) complex was identified, and in the solid state, the Ir(III) complex approved a distorted octahedral coordination environment. This study demonstrated that substituting a pyridine-formimidamide-based ligand as an ancillary ligand could alter the electronic properties of the Ir(III) complex, paving the way for a new method for creating an innovative blue emitter of the phosphorescent complex. Therefore, time-dependent density-functional theory calculations will be conducted to investigate the relationship between triplet states and emission spectra of the synthesised Ir(III) complex.

Acknowledgement

This research was conducted under the Fundamental Research Grant Scheme (FRGS/1/2019/STG01/UPSI/02/1) awarded by the Ministry of Education Malaysia. The authors would like to extend their thankfulness to Universiti Pendidikan Sultan Idris (UPSI) for the scientific support facilities, i-CRIM Universiti Kebangsaan Malaysia (UKM) for the X-ray crystallography, luminescence, and lifetime facilities, and INFRA Laboratory Universiti Malaya (UM) for the mass spectrometer facility.

References

1. Ho, C-L., Li, H. and Wong, W-Y. (2015). Red to near-infrared organometallic phosphorescent dyes for OLED applications. *Journal of Organometallic Chemistry*, 751: 261-285.
2. Costa, R. D., Orti, E., Bolink, H. J., Monti, F., Accorsi, G., and Armaroli, N. (2012). Luminescent ionic transition-metal complexes for light-emitting electrochemical cells. *Angew. Chemie - International Edition*, 51(33): 8178-8211.
3. Barbante, G. J., Doeven, E. H., Francis, P. S., Stringer, B. D., Hogan, C. F., Kheradmand, P. R., Wilson, D. J. D., and Barnard, P. J. (2015). Iridium(III) N-heterocyclic carbene complexes: An experimental and theoretical study of structural, spectroscopic, electrochemical and electrogenerated chemiluminescence properties. *Dalton Transaction*, 44(18): 8564-8576.
4. Yang, C-H., Mauro, M., Polo, F., Watanabe, S., Muenster, I., Fröhlich, R. and De Cola, L. (2012). Deep-blue-emitting heteroleptic iridium(III) complexes suited for highly efficient phosphorescent OLEDs. *Chemistry of Materials*, 24(19): 3684-3695.

5. Yanling, S., Shuai, Z., Godefroid, G., Jinghai, Y., and Zhijian, W. (2015). Modification of the emission colour and quantum efficiency for oxazoline and thiazoline containing iridium complexes via different NiO. *The Royal Society Chemistry*, 5(24): 18464-18470.
6. Ali, N. M., Ward, M. D., Hashim, N., and Daud, N. (2017). Synthesis and photophysical properties of bis(phenylpyridine) iridium(iii) dicyanide complexes. *Materials Research Innovation*, 23(3): 135-140.
7. Lee, S., and Han, W. S. (2020). Cyclometalated Ir(III) complexes towards blue-emissive dopant for organic light-emitting diodes: Fundamentals of photophysics and designing strategies. *Inorganic Chemistry Frontier*, 7(12): 2396-2422.
8. Adeloye, A. O., Mphahlele, M. J., Adekunle, A. S., Rhyman, L., and Ramasami, P. (2017). Spectroscopic, electrochemical and DFT studies of phosphorescent homoleptic cyclometalated iridium(III) complexes based on substituted 4-fluorophenylvinyland 4-methoxyphenylvinylquinolines. *Materials*, 10(10): 1061–1082.
9. Henwood, A. F., Pal, A. K., Cordes, D. B., Slawin, A. M. Z., Rees, T. W., Momblona, C., Babaei, A., Pertegás, A., Ortí, E., Bolink, H. J., Baranoff, E. and Zysman-Colman, E. (2017). Blue-emitting cationic iridium(III) complexes featuring pyridylpyrimidine ligands and their use in sky-blue electroluminescent devices. *Journal of Materials Chemistry C*, 5(37): 9638-9650.
10. Omae, I. (2016) Application of the five-membered ring blue light-emitting iridium products of cyclometalation reactions as OLEDs. *Coordination Chemistry Reviews,* 310: 154-169.
11. Tan, G., Wang, L., Wang, S., Liu, P., Fan, H., Ho, C-L., Ma, D. and Wong, W-Y. (2019). Synthesis, photoluminescence and electroluminescence of triphenylphosphine functionalized cyclometalated iridium(III) complexes. *Dyes and Pigments*, 160: 717-725.
12. Sheldrick, G. M. SAINT V4, Software reference m anual Siemens analytical X-ray systems. Madison, WI, USA; 1996
13. Sheldrick, G. M., SADABS, Program for empirical absorption correction of area detector data. German y: University of Göttingen, Göttingen, German, 19 96
14. Sheldrick, G. M. SHELXTL V5.1, Software refere nce manual, Bruker AXS, Madison, WI, USA, 199 7
15. Sajoto, T., Djurovich, P. I., Tamayo, A., Yousufud din, M., Bau, R., Thompson, M. E., Holmes, R. J . and Forrest, S. R. (2005). Blue and near-UV pho sphorescence from iridium complexes with cyclom etalated pyrazolyl or N-heterocyclic carbene liga nds. *Inorganic Chemistry*, 44(22): 7992-8003.
16. Bain, N. H. A. S., Ali, N. M., Juahir, Y., Hashim, N ., Isa, M. I., Mohamed, A., Kamari, A. and Yamin, B.M. (2021). Synthesis and spectroscopic studies o f phenylpyridine iridium(III) complexes with deriv atives of 1*h*-1,2,4-triazole as ancillary ligands. *Indonesian Journal of Chemistry*, 21(6): 1577-1585.
17. Robert, M. S., Francis, X. W. and David, J. K. (200 5). Spectrometric identification of organic compou nds. John Wiley & Sons, Inc., New York. Seventh E dition: pp. 72-204.
18. Pavia, D. L., Lampman, G. M., Kriz, G. S. and Vyvyan, J. R. (2015). Introduction to spectroscopy. Cengage Learning 200 First Stamford Place, Stamford, USA. Fifth Edition: pp. 14-329.
19. Gokce, H., Ozturk, N., Tasąn, M., Alpaslan, Y. B., Alpaslan, G., (2016). Spectroscopic characterization and quantum chemical computations of the 5-(4-pyridyl)-1-h-1,2,4-triazole-3-thiol molecule. *Spectroscopy Letters*, 49(3): 167-179.
20. Stringer, B. D., Quan, L. M., Barnard, P. J., Wilson, D. J. D. and Hogan, C. F. (2014). Iridium complexes of n-heterocyclic carbene ligands: investigation into the energetic requirements for efficient electrogenerated chemiluminescence. *Organometallics*, 33(18): 4860-4872.
21. Huynh, H. V.; Han, Y., Jothibasu, R. and Yang, J. A. (2009). ^{13}C NMR spectroscopic determination of ligand donor strengths using n-heterocyclic carbene complexes of palladium(II). *Organometallics*, 28(18): 5395-5404.

22. Sanner, R. D., Cherepy, N. J., Paul Martinez, H., Pham, H. Q. and Young Jr, V. G. (2019). Highly efficient phosphorescence from cyclometallated iridium(III) compounds: Improved syntheses of picolinate complexes and quantum chemical studies of their electronic structures. *Inorganica Chimica Acta,* 496: 119040-119078.
23. Donato, L., Abel, P. and Zysman-Colman, E. (2013). Cationic iridium(III) complexes bearing a bis(triazole) ancillary ligand. *Dalton Transactions*, 42(23): 8402-8412.
24. Xue, J., Xin, L. J., Hou, J. Y., Duan, L., Wang, R. J., Wei, Y. and Qiao, J. (2017). Homoleptic facial Ir(III) complexes via facile synthesis for high-efficiency and low-roll-off near-infrared organic light-emitting diodes over 750 nm. *Chemistry of Materials*, 29(11): 4775-4782.
25. Bain, N. H. A. S., Ali, N. M. Juahir, Y., Hashim, N., Isa, I. M., Mohamed, A., Kamari, A., Anouar, E. H., Yamin, B. M., Tajuddin, A. M. and Baharudin, M. H. (2020). Synthesis, crystal structure, photophysical properties, DFT studies and Hirshfeld surface analysis of a phosphorescent 1,2,4-triazole-based iridium(III) complex. *Polyhedron,* 188: 114690-114701.
26. Bain, N. H. A., Ali, N. M., Juahir, Y., Hashim, N., Isa, I. M., Mohamed, A., Kamari, A., and Yamin, B. M. (2018). Synthesis of phenylpyridine iridium(III) complexes with n-heterocyclic carbene as ancillary ligand. *IOP Conference Series Materials Science Engineering,* 440: 012010-012018.
27. Monti, F., Kessler, F., Delgado, M., Frey, J., Bazzanini, F., Accorsi, G., Armaroli, N., Bolink, H. J., Ort, E., Scopelliti, R., Nazeeruddin, M. K. and Baranoff, E. (2013). Charged bis-cyclometalated iridium(III) complexes with carbene-based ancillary ligands. *Inorganic Chemistry,* 52(18): 10292-10305.
28. Baranoff, E., Curchod, B. F. E., Monti, F., Steimer, F., Accorsi, G., Tavernelli, I., Rothlisberger, U., Scopelliti, R., Grätzel, M. and Nazeeruddin, M. K. (2012). Influence of halogen atoms on a homologous series of bis-cyclometalated iridium(III) complexes. *Inorganic Chemistry,* 51(2): 799-811.
29. Ryu, C. H., Lim, J., Kim, M. B., Lee, J. H., Hwang, H., Lee, J. Y., and Lee, K. M. (2021). Tris(5-phenyl-1h-1,2,4-triazolyl)iridium(III) complex and its use in blue phosphorescent organic light-emitting diodes to provide an external quantum efficiency of up to 27.8%. *Advanced Optical Materials,* 9(7): 1-7.
30. Tom, L., Diluzio, S., Hua, C. and Connell, T. U. (2022). Understanding the role of cyclometalating ligand regiochemistry on the photophysics of charged heteroleptic iridium(III) complexes. *Journal of Coordination Chemistry,* 75(11-14): 1722-1743.
31. Schneidenbach, D., Ammermann, S., Debeaux, M., Freund, A., Zöllner, M., Daniliuc, C., Jones, P. G., Kowalsky, W. and Johannes, H-H. (2010). Efficient and long-time stable red iridium(III) complexes for organic light-emitting diodes based on quinoxaline ligands. *Inorganic Chemistry*, 49(2): 397-406.